Materials Transactions, Vol. 48, No. 9 (2007) pp. 2340 to 2342

Fabrication and Characterization of GaP Photonic Crystals for Terahertz Wave Application

Kyosuke Saito*, Kei Nozawa*, Tadao Tanabe[1], Yutaka Oyama[1], Ken Suto[2], Jun-ichi Nishizawa[2], Tetsuo Sasaki[2], Tomoyuki Kimura[2]

[1]*Department of Materials Science, Graduate School of Engineering, Tohoku University, Sendai 980-8579, Japan*
[2]*Semiconductor Research Institute, Sendai 980-0845, Japan*

We have fabricated GaP two-dimensional photonic crystals (PCs) for terahertz (THz) wave generation by a reactive ion etching in Ar/Cl_2 gas chemistries. We performed 75-μm-deep etching of GaP, in which Al_2O_3 layer is applied as a hard mask with its selectivity as high as 125. We demonstrated the THz-wave generation from the fabricated GaP slab waveguide with the PC structure as a cladding layer under a collinear phase-matched difference frequency generation. In the frequency dependence of THz output power for the PC slab waveguide is seen at around 1.1 THz. From the in-plane transmission spectrum of THz-wave, we confirmed that the THz output characteristics had relation with the photonic structure for THz wave. [doi:10.2320/matertrans.MAW200728]

(Received April 24, 2007; Accepted May 21, 2007; Published July 11, 2007)

Keywords: *Terahertz-wave, GaP, Photonic crystal, optical waveguide, phonon-polariton, collinear phase matching*

1. Introduction

Terahertz (THz) frequency region between the radio and infrared frequencies has attracted a great deal of attention due to a number of important potential applications in medical and imaging fields.[1,2] Recent technological developments of coherent THz wave sources has realized these applications. The most THz-wave sources are based on photoconductive antenna, quantum cascade lasers, or non-linear optical effects such as difference frequency generation (DFG), optical parametric oscillation, and optical rectification.[3–17] The DFG can produce tunable, narrow linewidth, and high power THz-waves with ns-pulsed as well as CW operation.[18,19] The THz-waves can be generated at room temperature. The DFG is suitable for THz wave source of telecommunication, *in-situ* security screening.

A GaP crystal has been used to generated coherent THz-waves via the DFG process because of its transparent properties in the infrared and THz regions, while maintaining a relatively high efficiency for conversion due to a phonon-polariton excitation.[7–10,12–14,20] In addition, our previous works have generated THz-waves with bulk GaP crystals under a small-angle non-collinear phase matched DFG condition.[7–9] By using the THz wave source, a frequency-tunable THz spectrometer has constructed, and the THz spectra of important biomolecules (e.g. sugars, nucleosides, nucleotides, amino acids, etc.) were obtained.[21–23] By using GaP with waveguide structure as large as the wavelength of the THz wave, it is possible to generate THz-waves under a collinear $\chi^{(2)}$ phase-matching configuration with a simple optical system. Semiconductor Raman laser and amplifiers have also been demonstrated by using the waveguide effect. The waveguide structure allows to decrease the threshold pump power as low as 50 mW and a Raman gain is achieved to be $g = 12.3 \times 10^{-8}\,W{\cdot}cm^{-1}$ via the confinement of the phonon mode restricted in the GaP waveguides.[24,25] In THz-wave generation from GaP, we have also confirmed the enhancement of conversion efficiency by using the waveguide effect.[26]

Another effective method to improve conversion efficiency is to use artificial periodic structures. Recently, photonic crystals (PCs) have investigated due to their interesting properties and wide applications in many areas of science and industry. The PCs have been developed in the wide frequency from visible to microwave regions. For the optical region, PCs have been utilized in waveguides, high-Q filters, lasers, and fibers.[27–30] In THz region, PCs are also of interest, as they could contribute to improvement of THz technology. Comparing to applications of passive devices such as filters, waveguides and PC fibers, there are few active devices.[31–35]

In this study, we have fabricated GaP waveguide with two-dimensional photonic structure and demonstrated the THz-wave generation from the GaP slab waveguide with the PC structure as a cladding layer.

2. Fabrication of GaP PC Slab Waveguide

The GaP photonic crystal slab waveguide was fabricated in three steps as follows:

1) *Al_2O_3 mask fabrication*: An Al_2O_3 film of 500 nm thickness was deposited by electron-beam evaporation on the (001) semi-insulating GaP substrate with 300 μm thickness. This layer acts as a hard mask against a reactive ion etching of the GaP. Subsequently, a PC pattern was formed by lithography process with a g-line light.
2) *Reactive ion etching*: The GaP was etched using reactive ion etching in parallel plate discharge plasma. Plasma was generated by supplying 13.56 MHz rf power to the sample stage. A rf power of 100 W was supplied. Ar and Cl_2 gas chemistries were used as an etching gas. The flow rates of 0.5 (Ar) and 2.0 sccm (Cl_2) were controlled by mass flow controllers, respectively. The pressure of the process chamber became 4 Pa (30 mTorr).
3) *Removal of Al_2O_3 mask*: Using the buffered HF

*Graduate Student, Tohoku University

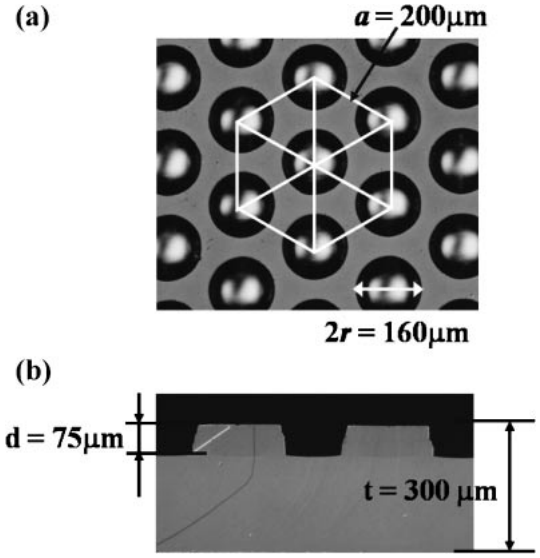

Fig. 1 Top (a) and cross-sectional (b) view of the fabricated GaP PC slab waveguide.

solution, the Al_2O_3 masking layer was removed and the sample was cleaved into the rectangle with 5 mm long in ⟨110⟩ direction and 10 mm wide in ⟨110⟩ direction.

Figure 1 shows the fabricated GaP photonic crystal slab waveguide. Figure 1 (a) is a top view of the surface. Air holes were arranged in a triangular lattice with a lattice constant a of 200 μm. The radius of air holes r was 80 μm. Figure 1 (b) is the cross-sectional view of the sample. A 30 minutes etching yielded an air hole depth of 75 μm. The etch rate reached 2.5 μm/min, and the etching selectivity was over 125. From the calculated result by a plane-wave expansion method, the photonic band gap was estimated in the frequency from 0.35 to 0.6 THz.

3. Experimental

Figure 2 shows the schematic of the experimental setup used for the THz-wave generation. A Q-switched Nd:YAG laser (1064-nm, 11 ns-pulse witdth,10-Hz repetition rate) was used as a signal beam, and a β-BaB_2O_4 (BBO)-based optical parametric oscillator (OPO) was used as the pump beam (6 ns-pulse width) in the DFG experiment. The OPO was tuned over the 1058–1063 nm range. The YAG and OPO input beams were carefully attenuated to 1.0 mJ and 0.5 mJ, respectively. In addition, the input beams were collimated to 1-mm diameter and directed along the ⟨110⟩ direction of GaP waveguide. The E-field polarization of the signal and pump beams was adjusted parallel to the ⟨110⟩ and ⟨001⟩ direction, respectively (TE and TM, respectively). The generated THz-wave was detected by a liquid helium cooled bolometer (Infrared Laboratories, Inc. USA) that had a typical response time of 100 μs and a sensitivity of 2.57×10^5 V/W. The bolometer signal was collected and measured with a digital oscilloscope.

4. Results and Discussion

The THz-wave generation was carried out under collinear

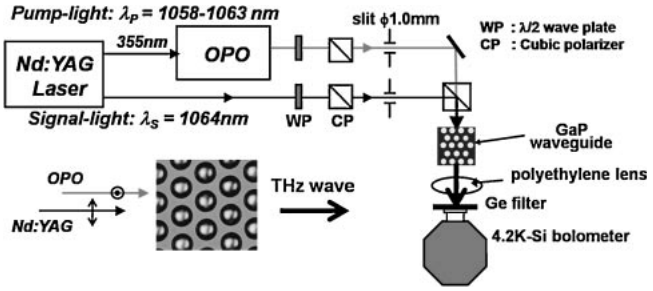

Fig. 2 Schematic drawing of the experimental set-up used for THz wave generation in GaP waveguides.

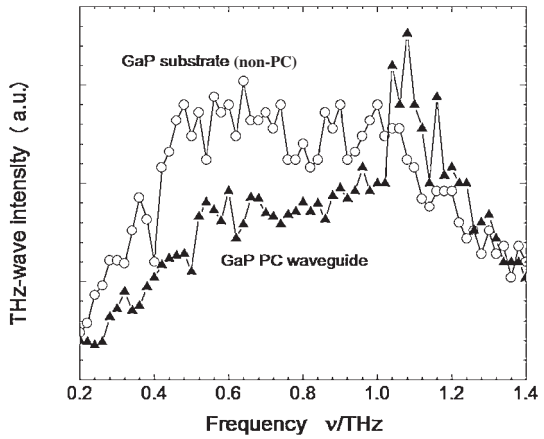

Fig. 3 Frequency dependence of the THz output power for unprocessed GaP slab waveguide (open circles) and PC patterned waveguide (solid triangles).

phase-matched DFG in GaP slab PC and non-PC waveguides. Figure 3 shows the output characteristics of the THz-wave generated from GaP slab waveguides, respectively. The frequency of OPO was varied against the fixed-frequency of the YAG source, THz output peak was observed around 0.8 THz for an unprocessed (non-PC) GaP slab waveguide. The bandwidth for half the maximum THz-wave output power was about 800 GHz. This bandwidth originated from the phase mismatch in the DFG process. The peak position and bandwidth were good agreement with calculated results based on waveguide theory.[36] On the other hand, the THz output showed different features for the PC patterned GaP slab waveguide: THz output peak was observed around 1.1 THz. The calculated peak frequency position is estimated 1.0 THz in case that PC layer is uniform cladding layer.

Figure 4 shows the in-plane THz-wave transmission characteristics of PC patterned waveguide along Γ-M direction. This measurement was carried out by the spectrometer using the GaP THz wave source.[21,22] The polarization of the incident THz wave was TE polarization. The transmission spectrum was normalized by that of the unprocessed GaP substrate. Solid curve is the result of a finite-difference time-domain (FDTD) simulation.

Several low transmission regions were appeared in this THz spectrum. One region from 0.4 to 0.6 THz is corresponding to the stop band in the PC structure. Around 0.9 THz, the photonic band gap is theoretically existed. It is noted that THz transmission increased around 1.1 THz. The

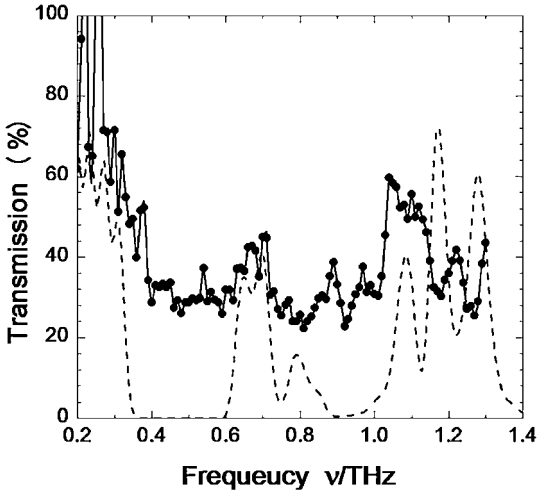

Fig. 4 THz transmission spectrum of the PC waveguide. Dashed curve is the FDTD simulation assuming the infinite PC thickness.

enhancement of THz wave generation shown in Fig. 3 is possible due to the higher transmission features around 1.1 THz. Some photonic band structure with low group velocity exists in this frequency region. These photonic bands affect the THz conversion efficiency.

5. Conclusions

We have fabricated GaP slab waveguide based two-dimensional photonic crystals (PCs) by the reactive ion etching in Ar/Cl_2 plasma chemistries. 75-μm-deep etching of GaP was performed by applying the Al_2O_3 hard mask with their selectivity as high as 125. THz wave generated from the fabricated GaP slab waveguide with the PC structure as a cladding layer. THz output power had relation with the transmittance of photonic waveguide for THz wave.

REFERENCES

1) J. Nishizawa: J. Acoust. Soc. Jpn **57** (2001) 163–169.
2) B. B. Hu and M. C. Nuss: Opt. Lett. **20** (1995) 1716–1718.
3) D. A. Auston, K. P. Cheung and P. R. Smith: Appl. Phys. Lett. **45** (1984) 284–286.
4) P. U. Jepsen, R. H. Jacobsen and S. R. Keiding: J. Opt. Soc. Am. B **13** (1996) 2424–2436.
5) M. Tani, S. Matsuura, K. Sakai and S. Nakashima: Appl. Opt. **36** (1997) 7853–7859.
6) J. Faist, F. Capasso, D. L. Sivco, C. Sirtori, A. L. Hutchinson and A. Y. Cho: Science **264** (1994) 553–556.
7) T. Tanabe, K. Suto, J. Nishizawa, T. Kimura and K. Saito: J. Appl. Phys. **93** (2003) 4610–4615.
8) T. Tanabe, K. Suto, J. Nishizawa, K. Saito and T. Kimura: Appl. Phys. Lett. **83** (2003) 237–239.
9) T. Tanabe, K. Suto, J. Nishizawa, K. Saito and T. Kimura: J. Phys. D: Appl. Phys. **36** (2003) 953–957.
10) F. De Martini: Phys. Rev. B **4** (1971) 4556–4578.
11) K. Kawase, M. Mizuno, S. Sohoma, H. Takahashi, T. Taniuchi, Y. Urata, S. Wada, H. Tashiro and H. Ito: Opt. Lett. **24** (1999) 1065–1067.
12) T. Taniuchi and H. Nakanishi: J. Appl. Phys. **95** (2004) 7588–7591.
13) W. Shi and Y. J. Ding: Opt. Lett. **30** (2005) 1030–1032.
14) I. Tomita, H. Suzuki, H. Ito, H. Takenouchi, K. Ajito, R. Rungsawang and Y. Ueno: Appl. Phys. Lett. **88** (2006) 071118 1–3.
15) K. Kawase, J. Shikata and H. Ito: J. Phys. D: Appl. Phys. **35** (2002) R1–R14.
16) X.-C. Zhang, Y. Jin and X. F. Ma: Appl. Phys. Lett. **61** (1992) 2764–2766.
17) A. Nahata, A. S. Weling and T. F. Heinz: Appl. Phys. Lett. **69** (1996) 2321–2323.
18) J. Nishizawa, T. Tanabe, K. Suto, Y. Watanabe, T. Sasaki and Y. Oyama: IEEE Photon. Technol. Lett. **18** (2006) 2008–2010.
19) T. Tanabe, J. Nishizawa, K. Suto, Y. Watanabe, T. Sasaki and Y. Oyama: Mater. Trans. **48** (2007) 980–983.
20) J. Nishizawa: Denshi Kagaku **14** (1963) 17–31 (in Japanese).
21) J. Nishizawa, T. Sasaki, K. Suto, T. Tanabe, K. Saito, T. Yamada and T. Kimura: Opt. Commun. **246** (2005) 229–239.
22) J. Nishizawa, K. Suto, T. Sasaki, T. Tanabe and T. Kimura: J. Phys. D: Appl. Phys. **36** (2003) 2958–2961.
23) J. Nishizawa, T. Sasaki, K. Suto, T. Tanabe, T. Yoshida, T. Kimura and K. Saito: Int. J. Infrared Milli. Waves **27** (2007) 779–789.
24) K. Suto, T. Kimura and J. Nishizawa: IEE Proc.- Optoelectron. **143** (1996) 113–118.
25) T. Saito, K. Suto, T. Kimura, A. Watanabe and J. Nishizawa: J. Appl. Phys. **87** (2000) 3399–3403.
26) J. Nishizawa, K. Suto, T. Tanabe, K. Saito, T. Kimura and Y. Oyama: IEEE Photon. Technol. Lett. **19** (2007) 143–145.
27) Y. Jiang, W. Jiang, L. Gu, X. Chen and R. T. Chen: Appl. Phys. Lett. **87** (2005) 221105.
28) S. Guo and S. Albin: Opt. Express **11** (2003) 1080–1089.
29) A. J. Danner, J. J. Raftery, P. O. Leisher and K. D. Choquette: Appl. Phys. Lett. **88** (2006) 091114.
30) T. A. Birks, D. Mogilevtsev, J. C. Knight and P. St. J. Russell: IEEE Photonics Technol. Lett. **11** (1999) 674–676.
31) T. D. Drysdale, I. S. Gregory, C. Baker, E. H. Linfield, W. R. Tribe and David R. S. Cumming: Appl. Phys. Lett. **85** (2004) 5173–5175.
32) K. Takagi, K. Seno and A. Kawasaki: Appl. Phys. Lett. **85** (2004) 3681–3683.
33) F. Miyamaru, M. Tanaka and M. Hangyo: Phys. Rev. B **74** (2006) 153416.
34) A. L. Bingham and D. Grischkowsky: Appl. Phys. Lett. **90** (2007) 091105.
35) G. Diwa, A. Quema, E. Estacio, R. Probre, H. Murakami, S. Ono and N. Sarukura: Appl. Phys. Lett. **87** (2005) 151114.
36) A. Yariv and P. Yeh: *Photonics*, (Oxford University Press, New York, 2007) pp. 110–126.